

Transverse-Momentum Distributions of Charged Particles Produced in $\bar{p}p$ Interactions at $\sqrt{s} = 630$ and 1800 GeV

F. Abe,⁽¹⁶⁾ D. Amidei,⁽³⁾ G. Apollinari,⁽¹¹⁾ G. Ascoli,⁽⁷⁾ M. Atac,⁽⁴⁾ P. Auchincloss,⁽¹⁴⁾ A. R. Baden,⁽⁶⁾ A. Barbaro-Galtieri,⁽⁹⁾ V. E. Barnes,⁽¹²⁾ F. Bedeschi,⁽¹¹⁾ S. Belforte,⁽¹¹⁾ G. Bellettini,⁽¹¹⁾ J. Bellinger,⁽¹⁷⁾ J. Bensinger,⁽²⁾ A. Beretvas,⁽¹⁴⁾ P. Berge,⁽⁴⁾ S. Bertolucci,⁽⁵⁾ S. Bhadra,⁽⁷⁾ M. Binkley,⁽⁴⁾ R. Blair,⁽¹⁾ C. Blocker,⁽²⁾ J. Bofill,⁽⁴⁾ A. W. Booth,⁽⁴⁾ G. Brandenburg,⁽⁶⁾ D. Brown,⁽⁶⁾ A. Byon,⁽¹²⁾ K. L. Byrum,⁽¹⁷⁾ M. Campbell,⁽³⁾ R. Carey,⁽⁶⁾ W. Carithers,⁽⁹⁾ D. Carlsmith,⁽¹⁷⁾ J. T. Carroll,⁽⁴⁾ R. Cashmore,⁽⁴⁾ F. Cervelli,⁽¹¹⁾ K. Chadwick,^(4,12) T. Chapin,⁽¹³⁾ G. Chiarelli,⁽¹¹⁾ W. Chinowsky,⁽⁹⁾ S. Cihangir,⁽¹⁵⁾ D. Cline,⁽¹⁷⁾ D. Connor,⁽¹⁰⁾ M. Contreras,⁽²⁾ J. Cooper,⁽⁴⁾ M. Cordelli,⁽⁵⁾ M. Curatolo,⁽⁵⁾ C. Day,⁽⁴⁾ R. DelFabbro,⁽¹¹⁾ M. Dell'Orso,⁽¹¹⁾ L. DeMortier,⁽²⁾ T. Devlin,⁽¹⁴⁾ D. DiBitonto,⁽¹⁵⁾ R. Diebold,⁽¹⁾ F. Dittus,⁽⁴⁾ A. DiVirgilio,⁽¹¹⁾ J. E. Elias,⁽⁴⁾ R. Ely,⁽⁹⁾ S. Errede,⁽⁷⁾ B. Esposito,⁽⁵⁾ A. Feldman,⁽⁶⁾ B. Flaugher,⁽¹⁴⁾ E. Focardi,⁽¹¹⁾ G. W. Foster,⁽⁴⁾ M. Franklin,^(6,7) J. Freeman,⁽⁴⁾ H. Frisch,⁽³⁾ Y. Fukui,⁽⁸⁾ A. F. Garfinkel,⁽¹²⁾ P. Giannetti,⁽¹¹⁾ N. Giokaris,⁽¹³⁾ P. Giromini,⁽⁵⁾ L. Gladney,⁽¹⁰⁾ M. Gold,⁽⁹⁾ K. Goulianos,⁽¹³⁾ C. Grosso-Pilcher,⁽³⁾ C. Haber,⁽⁹⁾ S. R. Hahn,⁽¹⁰⁾ R. Handler,⁽¹⁷⁾ R. M. Harris,⁽⁹⁾ J. Hauser,⁽³⁾ T. Hessing,⁽¹⁵⁾ R. Hollebeck,⁽¹⁰⁾ L. Holloway,⁽⁷⁾ P. Hu,⁽¹⁴⁾ B. Hubbard,⁽⁹⁾ P. Hurst,⁽⁷⁾ J. Huth,⁽⁴⁾ H. Jensen,⁽⁴⁾ R. P. Johnson,⁽⁴⁾ U. Joshi,⁽¹⁴⁾ R. W. Kadel,⁽⁴⁾ T. Kamon,⁽¹⁵⁾ S. Kanda,⁽¹⁶⁾ D. A. Kardelis,⁽⁷⁾ I. Karliner,⁽⁷⁾ E. Kearns,⁽⁶⁾ R. Kephart,⁽⁴⁾ P. Kesten,⁽²⁾ H. Keutelian,⁽⁷⁾ S. Kim,⁽¹⁶⁾ L. Kirsch,⁽²⁾ K. Kondo,⁽¹⁶⁾ U. Kruse,⁽⁷⁾ S. E. Kuhlmann,⁽¹²⁾ A. T. Laasanen,⁽¹²⁾ W. Li,⁽¹⁾ T. Liss,⁽³⁾ N. Lockyer,⁽¹⁰⁾ F. Marchetto,⁽¹⁵⁾ R. Markeloff,⁽¹⁷⁾ L. A. Markosky,⁽¹⁷⁾ P. McIntyre,⁽¹⁵⁾ A. Menzione,⁽¹¹⁾ T. Meyer,⁽¹⁵⁾ S. Mikamo,⁽⁸⁾ M. Miller,⁽¹⁰⁾ T. Mimashi,⁽¹⁶⁾ S. Miscetti,⁽⁵⁾ M. Mishina,⁽⁸⁾ S. Miyashita,⁽¹⁶⁾ N. Mondal,⁽¹⁷⁾ S. Mori,⁽¹⁶⁾ Y. Morita,⁽¹⁶⁾ A. Mukherjee,⁽⁴⁾ C. Newman-Holmes,⁽⁴⁾ L. Nodulman,⁽¹⁾ R. Paoletti,⁽¹¹⁾ A. Para,⁽⁴⁾ J. Patrick,⁽⁴⁾ T. J. Phillips,⁽⁶⁾ H. Piekarz,⁽²⁾ R. Plunkett,⁽¹³⁾ L. Pondrom,⁽¹⁷⁾ J. Proudfoot,⁽¹⁾ G. Punzi,⁽¹¹⁾ D. Quarrie,⁽⁴⁾ K. Ragan,⁽¹⁰⁾ G. Redlinger,⁽³⁾ J. Rhoades,⁽¹⁷⁾ F. Rimondi,⁽⁴⁾ L. Ristori,⁽¹¹⁾ T. Rohaly,⁽¹⁰⁾ A. Roodman,⁽³⁾ A. Sansoni,⁽⁵⁾ R. Sard,⁽⁷⁾ V. Scarpine,⁽⁷⁾ P. Schlabach,⁽⁷⁾ E. E. Schmidt,⁽⁴⁾ P. Schoessow,⁽¹⁾ M. H. Schub,⁽¹²⁾ R. Schwitters,⁽⁶⁾ A. Scribano,⁽¹¹⁾ S. Segler,⁽⁴⁾ M. Sekiguchi,⁽¹⁶⁾ P. Sestini,⁽¹¹⁾ M. Shapiro,⁽⁶⁾ M. Sheaff,⁽¹⁷⁾ M. Shibata,⁽¹⁶⁾ M. Shochet,⁽³⁾ J. Siegrist,⁽⁹⁾ P. Sinervo,⁽¹⁰⁾ J. Skarha,⁽¹⁷⁾ D. A. Smith,⁽⁷⁾ F. D. Snider,⁽³⁾ R. St. Denis,⁽⁶⁾ A. Stefanini,⁽¹¹⁾ Y. Takaiwa,⁽¹⁶⁾ K. Takikawa,⁽¹⁶⁾ S. Tarem,⁽³⁾ D. Theriot,⁽⁴⁾ A. Tollestrup,⁽⁴⁾ G. Tonelli,⁽¹¹⁾ Y. Tsay,⁽³⁾ F. Ukegawa,⁽¹⁶⁾ D. Underwood,⁽¹⁾ R. Vidal,⁽⁴⁾ R. G. Wagner,⁽¹⁾ R. L. Wagner,⁽⁴⁾ J. Walsh,⁽¹⁰⁾ T. Watts,⁽¹⁴⁾ R. Webb,⁽¹⁵⁾ T. Westhusing,⁽⁷⁾ S. White,⁽¹³⁾ A. Wicklund,⁽¹⁾ H. H. Williams,⁽¹⁰⁾ T. Yamanouchi,⁽⁴⁾ A. Yamashita,⁽¹⁶⁾ K. Yasuoka,⁽¹⁶⁾ G. P. Yeh,⁽⁴⁾ J. Yoh,⁽⁴⁾ and F. Zetti,⁽¹¹⁾

⁽¹⁾Argonne National Laboratory, Argonne, Illinois 60439

⁽²⁾Brandeis University, Waltham, Massachusetts 02254

⁽³⁾University of Chicago, Chicago, Illinois 60637

⁽⁴⁾Fermi National Accelerator Laboratory, Batavia, Illinois 60510

⁽⁵⁾Laboratori Nazionali di Frascati, Istituto Nazionale di Fisica Nucleare, Frascati, Italy

⁽⁶⁾Harvard University, Cambridge, Massachusetts 02138

⁽⁷⁾University of Illinois, Urbana, Illinois 61801

⁽⁸⁾National Laboratory for High Energy Physics (KEK), Tsukuba-gun, Ibaraki-ken 305, Japan

⁽⁹⁾Lawrence Berkeley Laboratory, Berkeley, California 94720

⁽¹⁰⁾University of Pennsylvania, Philadelphia, Pennsylvania 19104

⁽¹¹⁾Istituto Nazionale di Fisica Nucleare, University and Scuola Normale Superiore of Pisa, Pisa, Italy

⁽¹²⁾Purdue University, West Lafayette, Indiana 47907

⁽¹³⁾Rockefeller University, New York, New York 10021

⁽¹⁴⁾Rutgers University, Piscataway, New Jersey 08854

⁽¹⁵⁾Texas A&M University, College Station, Texas 77843

⁽¹⁶⁾University of Tsukuba, Ibaraki 305, Japan

⁽¹⁷⁾University of Wisconsin, Madison, Wisconsin 53706

(Received 8 June 1988; revised manuscript received 5 September 1988)

Measurements of inclusive transverse-momentum spectra for charged particles produced in proton-antiproton collisions at \sqrt{s} of 630 and 1800 GeV are presented and compared with data taken at lower energies.

PACS numbers: 13.85.Ni

We report measurements of the inclusive transverse-momentum spectra for charged particles produced in proton-antiproton collisions at the Fermilab Tevatron collider. Results were obtained at center-of-mass energies (\sqrt{s}) of 630 and 1800 GeV over the pseudorapidity range $|\eta| \lesssim 1$ with the Collider Detector at Fermilab (CDF). A comparison of our data with lower-energy data shows that the inclusive cross section at fixed momentum transverse to the beam axis (p_T) continues to increase rapidly with \sqrt{s} from 23 to 1800 GeV, especially for $p_T \gtrsim 1$ GeV/c.

At low \sqrt{s} ($\lesssim 15$ GeV) transverse-momentum spectra are described reasonably well by thermodynamic models¹ in which the invariant inclusive cross section falls exponentially. Fermilab,² CERN ISR,³ and CERN $S\bar{p}pS$ measurements^{4,5} show a significant departure from this form, suggesting an increased contribution due to hard scattering of partons. In parton models,⁶ power-law spectra modified by fragmentation functions and scaling violations are expected. In addition, the data^{4,7,8} show a slow growth with energy of the average transverse momentum for \sqrt{s} below 100 GeV and may indicate a more rapid growth at $S\bar{p}pS$ collider energies.

CDF is a large azimuthally symmetric general-purpose detector built to study $\bar{p}p$ collisions at the Tevatron collider. Details of CDF are described elsewhere⁹; the essential features relevant for this analysis are described below and shown in Fig. 1.

Beam-beam counters (BBC) were used for triggering. They consist of two sets of scintillation counters located at ± 5.82 m from the nominal interaction point and cover the pseudorapidity range $3.2 \lesssim |\eta| \lesssim 5.9$.

The vertex time-projection chamber (VTPC) is a set of eight time-projection-chamber models used to measure η for charged particles and to determine the event vertex position and overall topology. The acceptance of the VTPC depends on the position of the interaction but typically extends to $|\eta| = 3.5$.

The central tracking chamber (CTC) is a cylindrical drift chamber located in a 1.5-T magnetic field provided by a superconducting solenoid coaxial with the beam.

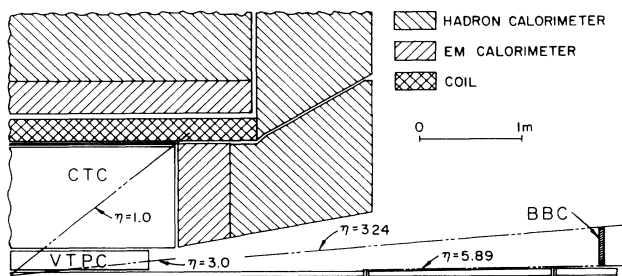


FIG. 1. Cross-sectional view through $\frac{1}{4}$ of CDF central detector.

The chamber has 86 layers of wires distributed over its 1.2-m radial thickness. The spatial resolution of each measurement was $< 300 \mu\text{m}$. For this analysis the transverse-momentum resolution, including multiple-scattering effects, was $\sigma_{p_T}/p_T^2 \lesssim 0.003 (\text{GeV}/c)^{-1}$ for $p_T > 2$ GeV/c and $|\eta| \lesssim 1$.

The event trigger required that at least one charged particle transverse each set of BBC in coincidence with the beam crossing. A sample of 55700 triggers at 1800 GeV and 9400 triggers at 630 GeV was collected. Proton-antiproton collisions were selected from this sample with reconstructed BBC and VTPC information. The distribution of collision vertices along the beam axis was Gaussian with a typical σ of 40 cm. The position of the interaction derived from the VTPC was required to be consistent with that determined from the BBC timing information. To ensure full acceptance of the VTPC for $|\eta| \lesssim 3$, events originating at $|z| > 65$ cm were rejected. Only events with at least four charged particles in the range $0 < |\eta| < 3$ and at least one particle in each hemisphere ($\eta > 0$, $\eta < 0$) were used. The fraction of triggers due to beam-gas interactions ranged from 4% to 50% depending upon luminosity. The instantaneous luminosity ranged from 2×10^{27} to $4 \times 10^{28} \text{ cm}^{-2} \text{ s}^{-1}$ at 1800 GeV and was $\sim 7 \times 10^{26} \text{ cm}^{-2} \text{ s}^{-1}$ during the single 630-GeV run. The contamination of misidentified beam-gas interactions in the final data sample was estimated to be less than 0.5% at 1800 GeV and less than 2.5% at 630 GeV.

Our normalization of the inclusive cross sections does not depend upon determination and integration of the instantaneous luminosity. Instead, the production cross sections for events which pass the above selection criteria were estimated with measurements from the UA4 experiment¹⁰ to be 43 ± 6 mb at 1800 GeV and 34 ± 3 mb at 630 GeV. The integrated luminosity was determined from these cross sections and the total number of events passing our trigger and selection criterion. Uncertainties in our estimates of these cross sections are the principal source of error in the overall normalization of the presented results.

Tracks were required to traverse all layers of the CTC, corresponding to $|\eta| \lesssim 1$, and to pass through the interaction vertex within the accuracy given by the measurement error and multiple scattering: 5 cm along the beam direction and $(0.5^2 + 0.7/p_T^2)^{1/2}$ cm in the transverse plane.

The track-reconstruction efficiency was determined by two independent models. First, simulated tracks of various momenta were superimposed on real events and reconstructed with the standard reconstruction program. Second, CTC information for 500 reconstructed events was displayed with an interactive program and mistakes made by the standard reconstruction were corrected. Efficiencies determined with the two methods agree. Charged particles with p_T less than 0.33 GeV/c spiral in-

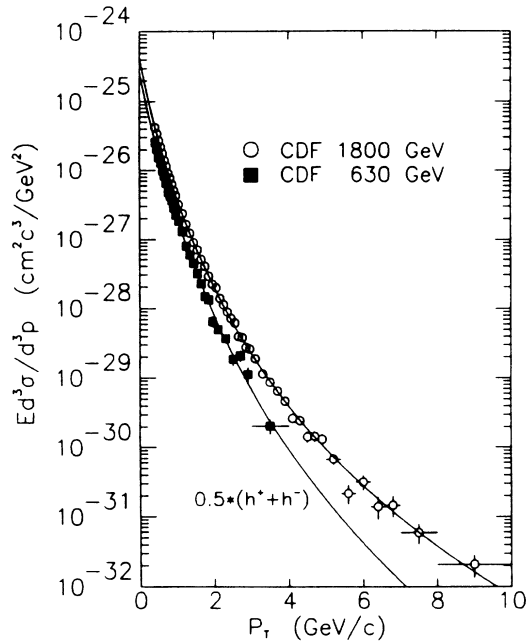


FIG. 2. Inclusive cross sections for rapidity $|y| < 1.0$ and fitted curves with p_0 fixed at $1.3 \text{ GeV}/c$.

side the solenoid. To ensure high and uniform reconstruction efficiency, only tracks with p_T above $0.4 \text{ GeV}/c$ were used. For this analysis the average reconstruction efficiency was $(99 \pm 1)\%$, independent of the vertex position, polar angle, and event multiplicity. The ratio of the transverse-momentum spectrum of positive particles to that of negative particles for $p_T > 0.4 \text{ GeV}/c$ is 1.00 ± 0.01 independent of p_T . All results are presented as the average of the spectra particles with both signs of charge.

The observed p_T spectrum was corrected for decays of charged pions and kaons, secondary interactions, photon conversions, and decays of neutral strange particles. The largest of these corrections was $< 5\%$. Misreconstruction of the trajectories of decaying charged pions and kaons were studied by reconstructing simulated decays

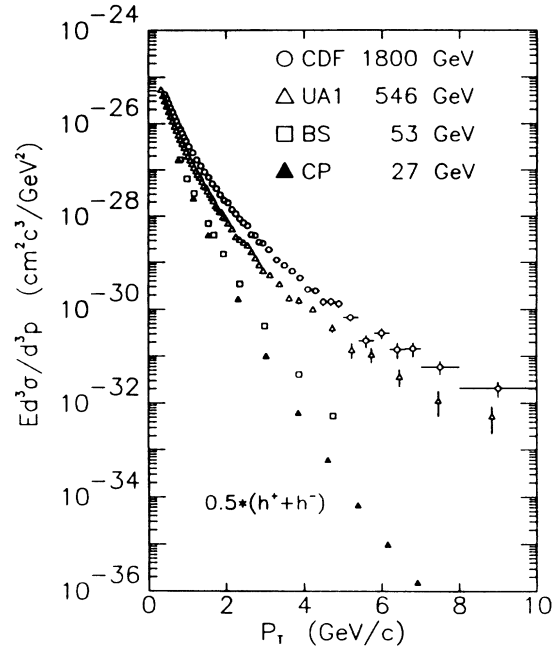


FIG. 3. Energy dependence of inclusive cross sections. Chicago-Princeton (CP) ($y=0$) Ref. 2, British-Scandinavian (BS) ($y=0$) Ref. 3, UA1 ($|y| < 2.5$) Ref. 7, and CDF ($|y| < 1.0$) collaborations.

and applying our acceptance cuts. The contribution from misreconstructed decays and the distortion of the spectrum due to finite momentum resolution were both negligible. Although for $p_T < 1 \text{ GeV}/c$ multiple-scattering and other systematic effects degrade the momentum resolution, it always remains very small compared to the bin size in p_T used for the spectrum. The overall correction was $< 2\%$ and nearly independent of p_T for $p_T > 0.5 \text{ GeV}/c$. The largest overall correction was 10% at $p_T = 0.4 \text{ GeV}/c$ where reconstruction efficiency corrections are largest. Invariant cross sections were calculated assuming all particles to be pions.

Our results are shown in Fig. 2. The shape of the inclusive cross section at 630 GeV agrees very well with

TABLE I. Fit parameters of $E d^3\sigma/d^3p = Ap^n/(p_T + p_0)^n$. Quoted errors are purely statistical.

\sqrt{s} (GeV)	Fit interval (GeV/c)	A [$10^{-24} \text{ cm}^2/(\text{GeV}^2/c^3)$]	p_0 (GeV/c)	n	χ^2	N_{DF}
1800	0.4-10.0	0.45 ± 0.01	1.29 ± 0.02	8.26 ± 0.08	102	64
	0.5-10.0	0.45 ± 0.01	1.29 ± 0.02	8.26 ± 0.07	90	62
	0.5-5.0	0.47 ± 0.01	1.25 ± 0.01	8.12 ± 0.05	86	59
630	0.4-4.0	0.27 ± 0.01	1.63 ± 0.13	10.2 ± 0.56	32	33
1800	0.4-10.0	0.45 ± 0.01	1.30 fixed	8.28 ± 0.02	103	65
630	0.4-4.0	0.33 ± 0.01	1.30 fixed	8.89 ± 0.06	39	34
546 (UA1)	0.3-2.0	0.46 ± 0.01	1.30 fixed	9.14 ± 0.02	29	32

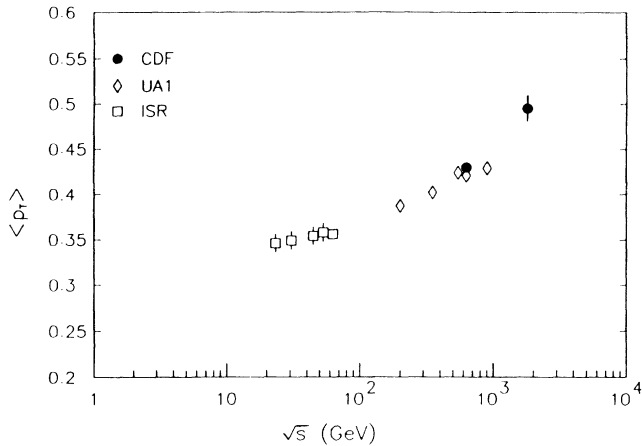


FIG. 4. Energy dependence of $\langle p_T \rangle$. UA1 results are averaged over jet and nonjet samples (Ref. 4); ISR values are averaged over particle types (Ref. 8).

the measurements of UA1 (Ref. 7) and UA2 (Ref. 5) at 546 GeV over the full range in p_T we present.

Figure 3 shows a comparison of inclusive cross sections measured at \sqrt{s} values from 27 to 1800 GeV. We find that the previously observed flattening in the shape of the p_T distribution with energy continues up to 1800 GeV.

Invariant cross sections were fitted with the functional form⁷

$$E \frac{d^3\sigma}{d^3p} = \frac{Ap_0^n}{(p_T + p_0)^n} \quad (1)$$

The fit parameters A , p_0 , n , and their statistical errors are given in Table I. Fitted curves are shown in Fig. 2. We find that p_0 and n are highly correlated. When fitting the data with p_0 fixed at 1.3 GeV/c, the power n decreases by 0.6 as the center-of-mass energy increases from 630 to 1800 GeV. Our result at 630 GeV, $n = 8.89 \pm 0.06$, is in reasonable agreement with the UA1 result at 546 GeV, $n = 9.14 \pm 0.02$.⁷ Results of the fits were stable against changes of the p_T range used in the fit.

Our determination of the mean value of transverse momentum $\langle p_T \rangle$ relies on the extrapolation of the observed spectrum to $p_T = 0$. The error in $\langle p_T \rangle$ due to uncertainty in the shape of the spectrum at low p_T was reduced by the use of constraints from the measurement of $dN/d\eta$. By integrating our fit to the inclusive spectrum for $p_T > 0.4$ GeV/c and subtracting this from $dN/d\eta$, we obtain $dN/d\eta$ for particles with $p_T < 0.4$ GeV/c. We then describe the low p_T portion of the inclusive spectrum with a function adjusted to the spectrum for 0.4 to 0.8 GeV/c and constrained to yield the correct $dN/d\eta$ for $p_T < 0.4$ GeV/c. By varying the functional form¹¹ of the p_T spectrum for $p_T < 0.4$ GeV/c with fixed $dN/d\eta$, the systematic error on $\langle p_T \rangle$ was estimated to be ~ 0.003

GeV/c. A preliminary analysis of VTPC data yields a ratio of $dN/d\eta$ at 1800 GeV to that at 630 GeV of 1.27 ± 0.04 . Interpolation of $dN/d\eta$ measurements¹² in the range 200 to 900 GeV gives $dN/d\eta = 3.30 \pm 0.15$ at 630 GeV for $\eta < 1$, in agreement with our own preliminary VTPC results of 3.2 ± 0.3 . Using these values we obtain $\langle p_T \rangle = 0.432 \pm 0.004$ GeV/c at 630 GeV and 0.495 ± 0.014 GeV/c at 1800 GeV. The estimated errors include uncertainties due to the extrapolation to $p_T = 0$, the value of the low- p_T cutoff, and in the ratio $dN/d\eta$. In addition, the 5% uncertainty in the value of $dN/d\eta$ at 630 GeV gives an additional error of 0.020 GeV/c common to both values of $\langle p_T \rangle$. We note that our result for $\langle p_T \rangle$ at 1800 GeV is in reasonable agreement with the result $\langle p_T \rangle = 0.46 \pm 0.01$ for particles below 3 GeV/c recently reported.¹³ Figure 4 shows that $\langle p_T \rangle$ grows significantly as a function of center-of-mass energy^{4,7,8} in our energy domain, in agreement with the trend observed in cosmic-ray interactions.¹⁴

The authors wish to thank the CDF technical support staff for their help and advice throughout the course of assembling and commissioning the detector. We are also indebted to the staff of the Tevatron collider for their hard and successful work in commissioning the machine for this first physics run. This work was supported by the Department of Energy; the National Science Foundation; Istituto Nazionale di Fisica Nucleare, Italy; the Ministry of Science, Culture, and Education of Japan; and A. P. Sloan Foundation.

¹R. Hagedorn, in *Cargèse Lectures in Physics*, edited by E. Schatzmann (Gordon and Breach, New York, 1973), Vol. 6, p. 643.

²D. Antreasyan *et al.*, Phys. Rev. D **19**, 764 (1979).

³B. Alper *et al.*, Nucl. Phys. **B87**, 19 (1975).

⁴F. Ceradini, in *Proceedings of the International Europhysics Conference on High Energy Physics, Bari, Italy, 18-24 July, 1985* (European Physical Society, Geneva, 1985), p. 363.

⁵M. Banner *et al.*, Phys. Lett. **122B**, 322 (1983); M. Banner *et al.*, Z. Phys. C **27**, 329 (1985).

⁶S. M. Berman *et al.*, Phys. Rev. D **4**, 3388 (1971).

⁷G. Arnison *et al.*, Phys. Lett. **118B**, 167 (1982).

⁸A. Rossi *et al.*, Nucl. Phys. **B84**, 269 (1975), and references therein.

⁹See F. Abe *et al.*, Nucl. Instrum. Methods Phys. Res., Sect. A **271**, 487 (1988), and references therein.

¹⁰D. Bernard *et al.*, Phys. Lett. B **186**, 227 (1987).

¹¹Forms used were $A \exp(-Bp_T)$, $A \exp(-Bp_T^2)$, $A + Bp_T + Cp_T^2$, and $Ap_0^n/(p_T + p_0)^n$.

¹²G. Ekspong, Nucl. Phys. **A461**, 145 (1987).

¹³T. Alexopoulos *et al.*, Phys. Rev. Lett. **60**, 1622 (1988).

¹⁴See, for example, C. Lattes *et al.*, Phys. Rep. **65**, 151 (1980).